TÜBİTAK

Turkish Journal of Chemistry

http://journals.tubitak.gov.tr/chem/

Research Article

Turk J Chem
(2022) 46: 523-529
© TÜBİTAK
doi:10.3906/kim-2110-22

A BODIPY based probe for the reversible "turn on" detection of Au(III) ions

Muhammed ÜÇÜNCÜ*
Department of Analytical Chemistry, Faculty of Pharmacy, İzmir Katip Çelebi University, İzmir, Turkey

Received: 11.10.2021 • **Accepted/Published Online:** 18.12.2021 • **Final Version:** 27.04.2022

Abstract: A new "turn on" fluorescent probe for the rapid and selective detection of Au^{3+} ions over other metal ions was developed. The probe design was constructed on a BODIPY-2-aminopyridine skeleton showing a weak fluorescence emission signal which increased substantially after the coordination of Au^{3+} ions. The probe displayed remarkable sensing performances such as a low limit of detection (17 nM), a short response time (<1 min), and ability in a wide range of pH's (6–11). The designed probe was found to have 2:1 coordination stoichiometry according to Job's plot analysis and most importantly to interact reversibly with Au^{3+} ions.

Key words: BODIPY, 2-aminopyridine, chemosensors, gold(III) ions, "turn on" sensing

1. Introduction

Gold has attracted great attention in various research fields, including chemistry, electronics, and medicine, due to its unique photochemical and photophysical properties. The outstanding catalytic activity of gold ions (Au^{+} and Au^{3+}) allows the progress of many complex organic transformations [1–3]. In addition, its high electrical conductivity, chemical inertness, and malleability increase its significance for electronics applications [4]. In addition to these positive features, the nanoparticle forms of gold have been frequently used in biological systems for imaging applications and drug delivery systems [5,6]. Moreover, gold is present in the structure of many drugs that have been used to treat several significant diseases including rheumatoid arthritis, cancer, AIDS, bronchial asthma, and malaria [7–9]. However, the accumulation of gold ions in living organisms has been previously reported to show high toxicity due to strong interactions with biomolecules (e.g., DNA, enzymes, etc.) [10,11]. Therefore, the development of both sensitive and selective methods to detect gold ions is in high demand.

Recently, fluorometric methods which rely on the changes in fluorescence signal in the presence of target analyte have gained substantial attention for trace metal analysis [12–16]. They offer high sensitivity and selectivity, ease of applicability in solution and biological systems and relatively cheap instrumentation which all together make fluorescent probes excellent alternatives to traditional analytical methods such as inductively coupled plasma atomic emission spectroscopy (ICP-AAS), ICP optical emission spectroscopy (ICP-OES), and ICP mass spectroscopy.

Several fluorescent probes have been specifically designed to detect gold ions by utilizing fluorophores including BODIPY [17,18], Rhodamine [19–20], fluorescein [21–23], coumarin [24], and naphthalimide [25]. Most of these probes were constructed on irreversible reaction-based sensing strategies that are largely based on the alkynophilic character of gold ions [17, 19, 24] or hydrolysis of C = N bond [21, 26, 27]. However, both strategies have some drawbacks, such as the potential cross-reactivity of other metal ions with alkynophilic/Lewis acidic character which might interfere with gold ion sensing. Another approach in probe design is to construct the reversible coordination of gold ions to heteroatom-containing ligands. However, there are only a few studies in the literature that have reported the use of the latter type of probes because of the difficulties in the design and synthesis of single analyte selective ligands [28–30].

Herein, the design, synthesis, and spectral characteristics of a new "turn on" fluorescent molecular probe, BOD-AP, for the selective and sensitive detection of Au^{3+} ions in an aqueous environment have been presented. BODIPY dye was selected as a signal reporter unit due to its exceptional properties such as high fluorescence quantum yield, high extinction coefficient, high photo-stability, and robustness towards chemicals. BODIPY was decorated with a 2-aminopyridine receptor unit bearing heteroatoms that enable the coordination of gold ions. BOD-AP was designed to be a nonfluorescent ("*off mode*") probe in its initial state due to the photo-induced electron transfer and to convert into fluorescent ("*on mode*") after the coordination of Au^{3+} ions.

* Correspondence: muhammed.ucuncu@ikc.edu.tr

2. Materials and methods

2.1. General methods

All reagents were purchased from Sigma-Aldrich and used without further purification. ^{1}H NMR and ^{13}C NMR were measured on a VNMRJ 600 nuclear magnetic resonance spectrometer (Varian Inc., Palo Alto, CA, USA). The mass analysis was conducted with Thermo Q-Exactive Orbitrap device (Thermo Fisher Scientific Inc., Waltham, MA, USA). The melting point was determined by using the Electrothermal Melting Point Apparatus 9200. UV-vis absorption and fluorescence emission spectra were obtained using a Shimadzu 1900i spectrophotometer and Varian Cary Eclipse fluorescence spectrophotometer (Varian Inc.), respectively. Quantum yield measurements were conducted with Hamamatsu Quantaurus-QY Absolute PL quantum yield spectrometer. The pH values were adjusted by using the HI-8014 (HANNA) pH meter.

2.2. Fluorescence measurements

The stock solution of BOD-AP (1 mM) was prepared in ethanol and diluted to proper concentrations for each measurement by using different ratios of 0.1 M phosphate buffer/ethanol (total sample volume = 2 mL). The stock solutions of metal ions (20 mM) were prepared by dissolving their nitrate and chloride salts in deionized water. For each measurement, proper volumes from the stock solution of metal ions were added to a probe solution (10 μM, 2 mL) that was contained in a quartz cuvette with 10 mm path length. Upon excitation at 460 nm, the fluorescence emission spectra were collected between 480–700 nm. In all measurements, the slit width for both excitation and emission were kept at 2.5 nm. All measurements were conducted in triplicate at least.

2.3. Synthesis of BOD-AP

Meso-chloromethyl-BODIPY (meso-BOD-Cl) was prepared as previously reported [31]. The probe molecule, BOD-AP, was synthesized using a slightly modified version of protocol reported by Xu et al. [32]. To a solution of meso-BOD-Cl (100 mg, 0.34 mmol) in tetrahydrofuran (50 mL) 2-aminopyridine (32 mg, 0.34 mmol), and K_2CO_3 (64 mg, 0.4 mmol) were added, and the solution was stirred for 5 h under nitrogen atmosphere at reflux temperature. The progress of the reaction was monitored by TLC and cooled to room temperature when all starting materials consumed. THF was removed under reduced pressure and resulting mixture was extracted with dichloromethane (3 × 100 mL). The collected organic layers were combined and washed with brine, then dried over Na_2SO_4, filtered and solvents removed under reduced pressure. The crude mixture purified by silica gel chromatography (Hexane:DCM, 3:1, v/v) and title compound, BOD-AP, was obtained as orange solid (84.3 mg, 70%). Mp: 203–205 °C. ^{1}H NMR (600 MHz, $CDCl_3$, δ, ppm) δ 8.11 (d, J = 4.2 Hz, 1H), 7.38 (t, J = 7.2 Hz, 1H), 6.57 (t, J = 7.2 Hz, 1H), 6.42 (d, J = 8.4 Hz, 1H), 6.24 (s, 1H), 6.10 (s, 1H), 5.18 (s, 1H), 4.79 (d, J = 6.6 Hz, 2H), 2.58 (s, 3H), 2.54 (s, 3H), 2.42 (s, 3H), 2.37 (s, 3H). ^{13}C NMR (150 MHz, $CDCl_3$, δ, ppm) δ 158.6, 155.6, 153.6, 148.2, 142.7 (2×C), 140.5, 137.6, 132.9, 132.2, 122.2, 119.7, 113.4, 107.4, 39.3, 17.6 (2×C), 16.7, 14.7. Calcd for $C_{19}H_{21}BF_2N_4$: 354.18273 $[M]^+$, found: 355.18954 $[M + H]^+$.

3. Results and discussion

The title compound, BOD-AP was obtained by following the synthetic route outlined in Scheme 1. The meso-BOD-Cl was prepared as previously reported [31] and treated with the commercially available 2-aminopyridine to give BOD-AP as an orange solid with a good reaction yield (70%). The structure of BOD-AP was confirmed by ^{1}H and ^{13}C NMR spectroscopy and HRMS analysis.

The aromatic protons resonated in the range of 8.11 ppm and 6.10 ppm in the ^{1}H NMR spectra proved the presence of a pyridine ring on the probe structure. The NH proton showed a broad singlet peak centred at 5.18 ppm, and the methylene protons resonated at 4.79 ppm which is split into a doublet due to the low exchange rate of proton on the neighbouring nitrogen proton [33, 34]. The obtained spectral profile clearly demonstrated that the nucleophilic substitution

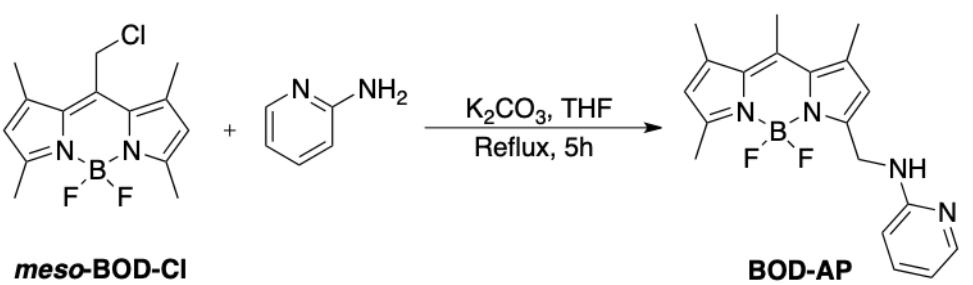

Scheme 1. Synthetic route to BOD-AP.

of 2-aminopyridine to the BODIPY core took place at the 3-methyl position instead of at the meso position. As reported in the literature, four methyl groups of meso substituted products must have appeared as two singlets (each peak 6H) [32]. However, in obtained ^{1}H NMR spectra, the presence of four singlet peaks for methyl groups (each centred at 2.58 ppm, 2.54 ppm, 2.42 ppm, 2.37 ppm) was clear evidence of the position that the nucleophile substituted at 3-position.

The optimization studies of sensing conditions for Au^{3+} ion detection were performed by the investigation of the effect of several parameters including a solvent/buffer type, water ratio, pH, and time. Owing to the hydrophobic core structure of BOD-AP, the addition of an organic cosolvent was required to prevent any aggregation in the solution. In this regard, EtOH-H_2O (1/1, v/v) and CH_3CN-H_2O (1/1, v/v) mixtures buffered at pH 7.0 by HEPES (HEP), phosphate buffer (PB), or PBS were screened. As shown in Figure 1a, the addition of Au^{3+} (2 equiv.) to the BOD-AP solutions (10 μM in EtOH-H_2O and CH_3CN-H_2O mixtures buffered at pH 7.0 by phosphate buffer (0.1 M)) resulted in the same fold increase in the fluorescence signal at 511 nm. Because of its low toxicity and commercial availability, ethanol was selected as a cosolvent to perform further fluorescence measurements. In addition, the effect of the water percentage was investigated where 1:1 (v/v) EtOH/H_2O ratio was determined as optimal condition (pH 7.0, 0.1 M phosphate buffer) (Figure 1b).

The receptor unit is prone to protonation under acidic conditions (pH 2-5). Therefore, BOD-AP exhibited a strong fluorescence signal (protonation cancels the effect of PET quenching) at this pH range and a negligible increase was observed in the presence of Au^{3+} ions (2 equiv.). At physiological or higher pH values, the receptor unit enables the quench fluorophore over PET mechanism and the addition of Au^{3+} ions, thus resulting in a remarkable increase in fluorescence emission (Figure 1c). After the careful examination of all parameters, the optimal sensing conditions were established as 10 μM BOD-AP in 0.1 M phosphate buffer/EtOH (pH 7.0, 1:1, v/v).

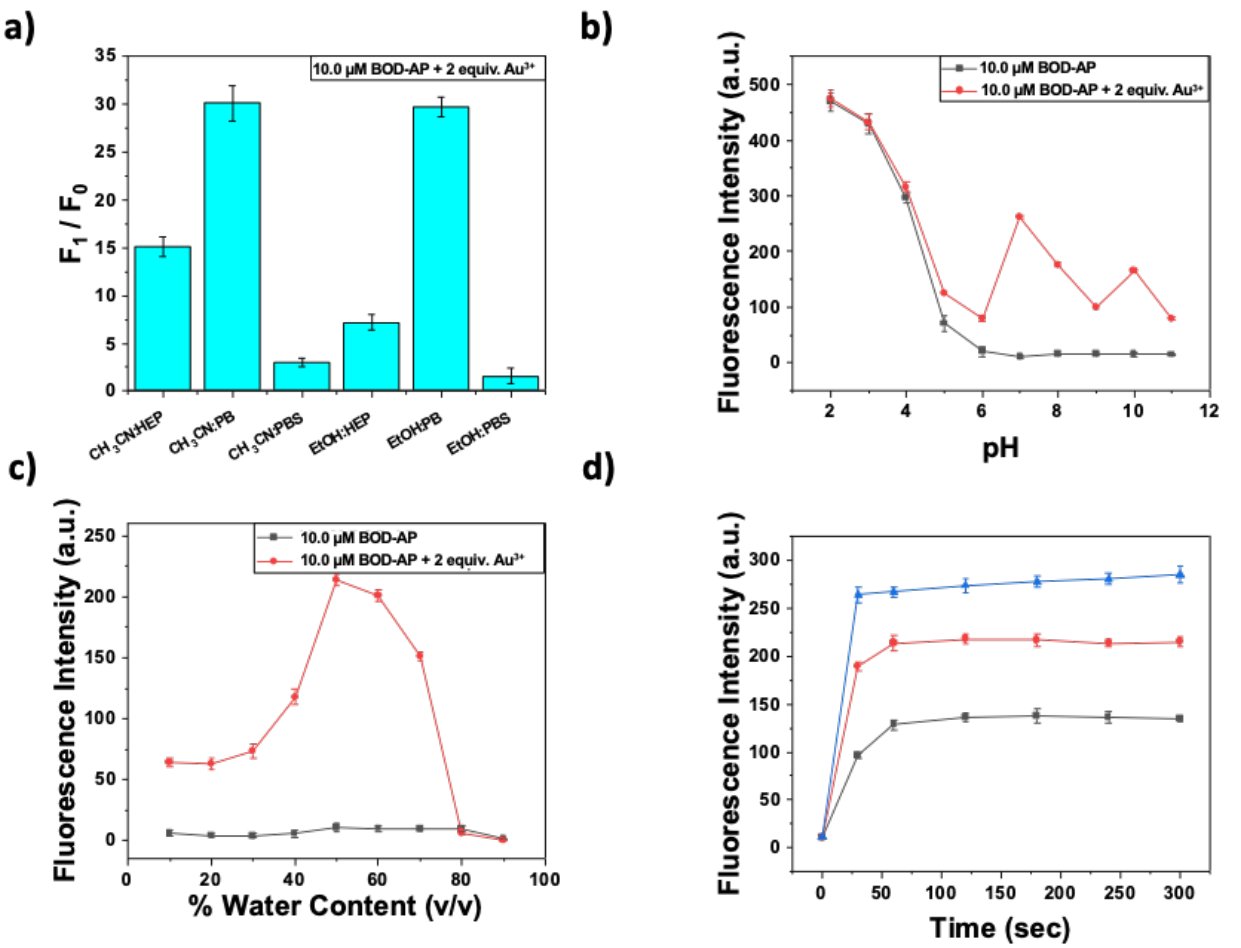

Figure 1. Optimization of sensing conditions BOD-AP for Au^{3+} ion sensing. The effect of a) solvent/buffer type b) water content (%, v/v) c) pH on Au^{3+} sensing event (BOD-AP (10 μM) + Au^{3+} (20 μM)) d) time profile of interaction of BOD-AP (10 μM) with Au^{3+} [5 (▪), 10 (●) and 20 (▲) μM.] in 0.1 M phosphate buffer/EtOH (pH 7.0, v/v, 1:1) (λ_{ex} = 460 nm, λ_{em} = 511 nm at 25 °C).

The spectral characteristics of BOD-AP were investigated by using UV-vis and fluorescence spectroscopy. BOD-AP has an absorption band at 497 nm which remained unchanged after the addition of Au^{3+} ions (Figure 2). As expected, the probe showed a very weak fluorescence emission ($F_F = 0.002$) centred at 509 nm due to the PET quenching process. Upon the addition of increasing concentrations of Au^{3+} ions (0.2 to 20 μM) a linear increase in fluorescence emission with a very small red shift (λ_{em} = 511 nm) was observed (Figure 3). The saturation point in the fluorescence was achieved by the addition of 2 equiv. of Au^{3+} with a 29-fold signal enhancement ($F_F = 0.88$). The fluorescence titration experiment revealed that the minimum detectable amount of Au^{3+} ions is 17 nM based on the signal-to-noise ratio (S/N = 3) (Figure S1). It is also important to note that the spectral response of the probe towards Au^{3+} ions was extremely fast, reaching maximum levels within only a min (Figure 1d).

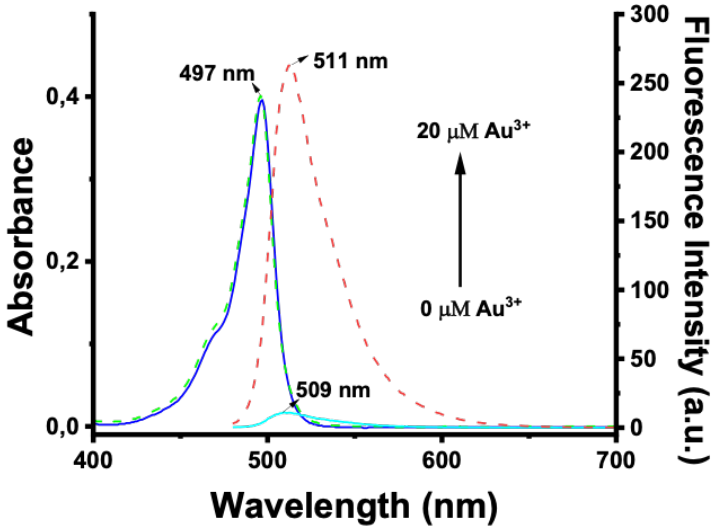

Figure 2. Absorbance spectra of BOD-AP (10 μM) in the absence (blue solid-line) and presence (green dot-line) of 2 equiv. (20 μM) of Au^{3+} and fluorescence spectra of BOD-AP (10 μM) in the absence (cyan solid-line) and presence (red dot-line) of 2 equiv. (20 μM) of Au^{3+} in 0.1 M phosphate buffer/EtOH (pH = 7.0, v/v, 1:1).

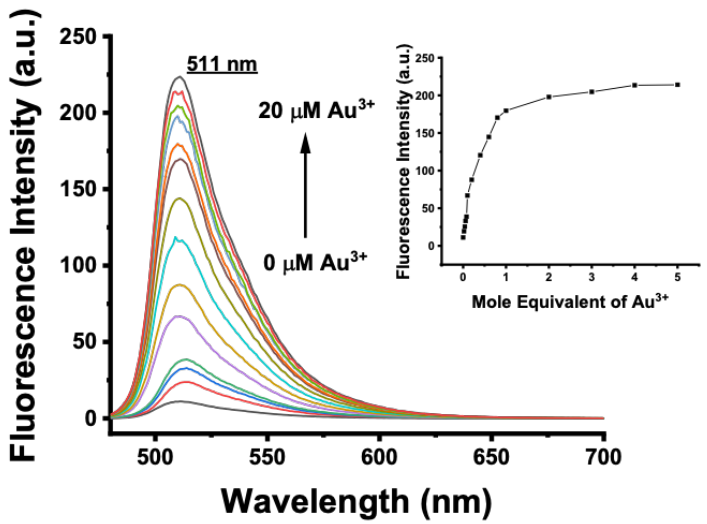

Figure 3. Fluorescence spectra of BOD-AP (10 μM) in the presence of increasing concentrations of Au^{3+} (0-20 μM, 0-2 equiv.) in a 0.1 M phosphate buffer/EtOH (pH = 7.0, 1:1, v/v) (λ_{exc} = 460 nm at 25 °C). Inset: Calibration curve.

To evaluate the selectivity profile of the probe, excess amounts of other metal ions (including Na^{+}, K^{+}, Li^{+}, Ca^{2+}, Mg^{2+}, Ba^{2+}, Ag^{+}, Hg^{2+}, Zn^{2+}, Pb^{2+}, Ni^{2+}, Cd^{2+}, Fe^{2+}, Cr^{3+}, Ce^{3+}, and Al^{3+}) were added to the BOD-AP solution (10 μM) and then the changes in the fluorescence signals were recorded. BOD-AP did not show any significant response towards the addition of excess amounts (100 μM, 10 equiv.) of any other metal cations (Figure 4a).

Moreover, the possible interference of these species was investigated by the addition of Au^{3+} ions (2 equiv.) to the solution of BOD-AP (10 μM) treated by an excess of other metal cations (100 μM, 10 equiv.). The performed study resulted in only negligible changes in the fluorometric response of the probe to Au^{3+} ions (Figure 4b). These results clearly demonstrate that the probe allows the selective detection of Au^{3+} ions in the presence of any other competitive species. Furthermore, to investigate the applicability of the sensing system in the more complex sensing media, the combination of the potentially interfering metal cations was added into the probe solution. The probe remained silent in the presence of these cations and signal enhancement was only observed upon after the addition of Au^{3+} ions (2 equiv.) (Figure S4).

The mechanism and stoichiometry of the sensing event were explored by a reversibility experiment and Job's plot analysis (Scheme 2). As shown in Figure S2, the treatment of BOD-AP with 2 equiv. of Au^{3+} ions reduced the effect of the PET mechanism, and a strong fluorescence emission band at 511 nm was observed. To reverse this, Na_2S (2 equiv.) which has a high affinity to Au^{3+} ions was added to the BOD-AP + Au^{3+} solution. The immediate decrease in the fluorescence signal down to its original intensity confirmed the reversibility of the sensing event. In addition, Job's plot analysis based on fluorescence titration experiment results revealed the 2:1 stoichiometry between BOD-AP and Au^{3+} ions for the complexation process (Figure S3).

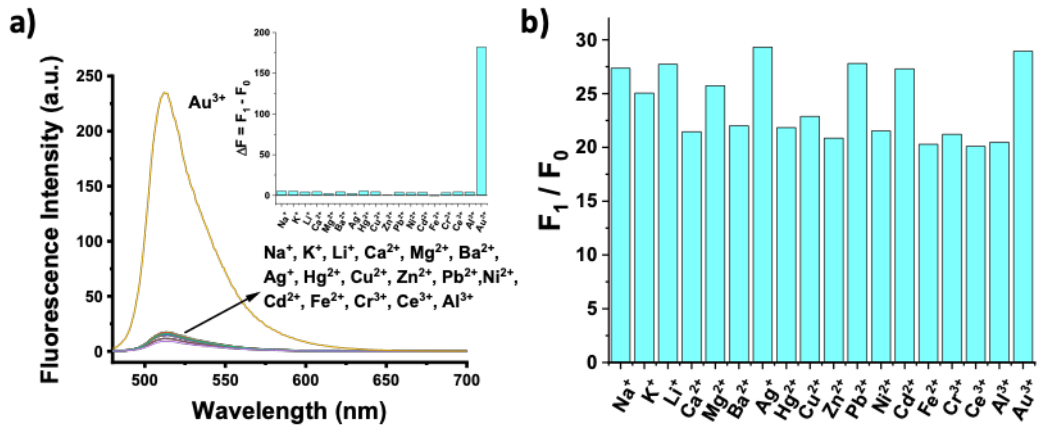

Figure 4. a) Fluorescence spectra of BOD-AP (10 μM), BOD-AP (10 μM) + Au^{3+} (20 μM, 2 equiv.), BOD-AP (10 μM) + other ions (100 μM, 10 equiv.) in 0.1 M phosphate buffer, pH 7.0/EtOH (v/v, 1:1) (λ_{ex}: 460 nm, at 25 °C). Inset: Bar graph notation. b) Fluorescence intensities of BOD-AP (10 μM) in the presence of Au^{3+} (20 μM, 2 equiv.) and 10 equiv. of other metal ions in 0.1 M phosphate buffer, pH 7.0/EtOH (v/v, 1:1) (λ_{ex} = 460 nm, λ_{em} = 511 nm at 25 °C).

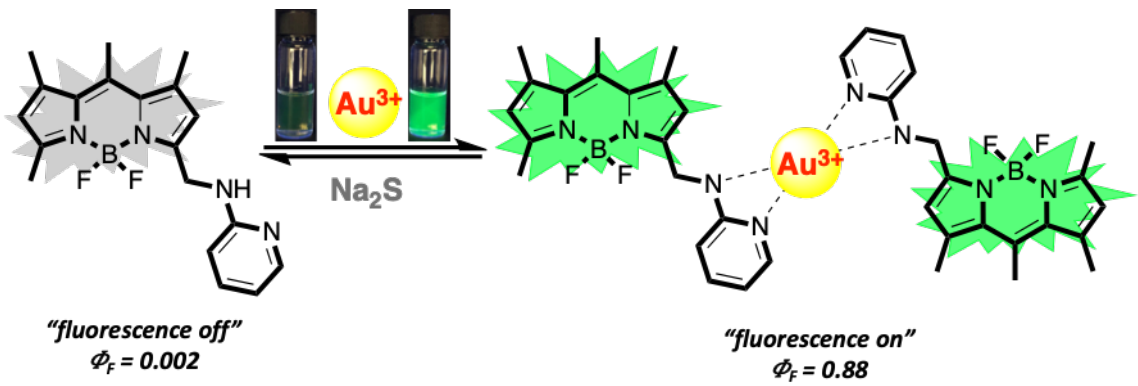

Scheme 2. Reversible sensing mechanism of BOD-AP with Au^{3+}.

In conclusion, synthesis, characterization, and spectral behaviours of a new fluorescent chemosensor that enables the detection of Au^{3+} ions in an aqueous environment were reported. The probe displayed a rapid (<1 min) "turn on" fluorescence response towards Au^{3+} ions with high selectivity and sensitivity (17 nm LoD). In addition, the designed probe showed 2:1 coordination stoichiometry and most importantly reversible interaction with gold ions.

Acknowledgment
The author gratefully acknowledges Erman Karakuş, Eda Erdemir, and Garen Suna for characterization studies.

References

1. Shahzad SA, Sajid MA, Khan ZA, Canseco-Gonzalez D. Gold catalysis in organic transformations: A review. Synthetic Communications 2017; 47 (8): 735-755. doi: 10.1080/00397911.2017.1280508

2. Campeau D, Rayo DFL, Mansour A, Muratov K, Gagosz F. Gold-catalyzed reactions of specially activated alkynes, allenes, and alkenes. Chemical Reviews 2021; 121 (14): 8756-8867. doi: 10.1021/acs.chemrev.0c00788

3. Zheng Z, Ma X, Cheng X, Zhao K, Gutman K et al. Homogeneous gold-catalyzed oxidation reactions. Chemical Reviews 2021; 121 (14): 8979–9038. doi: 10.1021/acs.chemrev.0c00774

4. Goodman P. Current and future uses of gold in electronics. Gold Bulletin 2002; 35: 21-26. doi: 10.1007/BF03214833

5. Kong FY, Zhang JW, Li RF, Wang ZX, Wang WJ et al. Unique roles of gold nanoparticles in drug delivery, targeting and imaging applications. Molecules 2017; 22 (9): 1445. doi: 10.3390/molecules22091445

6. Mohd-Zahid MH, Mohamud R, Abdullah CAC, Lim J, Alem H et al. Colorectal cancer stem cells: A review of targeted drug delivery by gold nanoparticles. RSC Advances 2020; 10 (2): 973-985. doi: 10.1039/C9RA08192E

7. Shaw III CF. Gold-based therapeutic agents. Chemical Reviews 1999; 99 (9): 2589 – 2600. doi: 10.1021/cr980431o

8. Yeo CI, Ooi KK, Tiekink ERT. Gold-based medicine: A paradigm shift in anti-cancer therapy? Molecules 2018; 23(6): 1410. doi: 10.3390/molecules23061410

9. Balfouriera A, Kolosnjaj-Tabib J, Luciania N, Carna F, Gazeau F. Gold-based therapy: From past to present. The Proceedings of the National Academy of Sciences 2020; 117 (37): 22639-22648. doi: 10.1073/pnas.2007285117

10. Connor EE, Mwamuka J, Gole A, Murphy CJ, Wyatt MD. Gold nanoparticles are taken up by human cells but do not cause acute cytotoxicity. Small 2005; 1 (3): 325-327. doi: 10.1002/smll.200400093.

11. Nyarko E, Hara T, Grab DJ, Habib A, Kim Y et al. In vitro toxicity of palladium(II) and gold(III) porphyrins and their aqueous metal ion counterparts on Trypanosoma brucei brucei growth. Chemico-Biological Interactions 2004; 148 (1-2): 19-25. doi: 10.1016/j.cbi.2004.03.004.

12. Carter KP, Young AM, Palmer AE. fluorescent sensors for measuring metal ions in living systems. Chemical Reviews 2014; 114 (8): 4564-4601. doi: 10.1021/cr400546e

13. Singha S, Kim D, Seo H, Cho WC, Ahn KH. Fluorescence sensing systems for gold and silver species. Chemical Society Reviews 2015; 44 (13): 4367-4399. doi: 10.1039/C4CS00328D

14. Wu D, Sedgwick AC, Gunnlaugsson T, Akkaya EU. Yoon J et al. Fluorescent chemosensors: the past, present and future. Chemical Society Reviews 2017; 46 (23): 7105-7123. doi: 10.1039/C7CS00240H

15. Kwon N, Hu Y, Yoon J. Fluorescent chemosensors for various analytes including reactive oxygen species, biothiol, metal ions, and toxic gases. ACS Omega 2018; 3(10): 13731-13751. doi: 10.1021/acs.chemrev.0c00774

16. Wu D, Chen L, Lee W, Ko G, Yin J et al. Recent progress in the development of organic dye based near-infrared fluorescence probes for metal ions. Coordination Chemistry Reviews 2018; 354: 74-97. doi: 10.1016/j.ccr.2017.06.011

17. Ucuncu M, Karakus E, Emrullahoglu M. A BODIPY-based fluorescent probe for ratiometric detection of gold ions: utilization of Z-enynol as the reactive unit. Chemical Communications 2016; 52 (53): 8247-8250. doi: 10.1039/C6CC04100K

18. Wang EZ, Pang LF, Zhou YM, Zhang JL, Yu F et al. A high-performance Schiff-base fluorescent probe for monitoring Au3+ in zebrafish based on BODIPY. Biosensors and Bioelectronics 2016; 77: 812–817. doi: 10.1016/j.bios.2015.10.051

19. Emrullahoglu M, Karakus E, Ucuncu M. A rhodamine based "turn-on" chemodosimeter for monitoring gold ions in synthetic samples and living cells. Analyst 2013; 138 (13): 3638-3641. doi: 10.1039/C3AN00024A

20. Pitsanuwong C, Boonwan J, Chomngam S, Wechakorn K, Kanjanasirirat P et al. A Rhodamine-based fluorescent chemodosimeter for Au^{3+} in aqueous solution and living cells. Journal of Fluorescence 2021; 31 (4): 1211-1218. doi: 10.1007/s10895-021-02725-0.

21. Kambam S, Wang BH, Wang F, Wang Y, Chen HY et al. A highly sensitive and selective fluorescein-based fluorescence probe for Au^{3+} and its application in living cell imaging. Sensors and Actuators B Chemical 2015; 209: 1005-1010. doi: 10.1016/j.snb.2014.12.085.

22. Cetintas C, Karakus E, Ucuncu M, Emrullahoglu M. A fluorescein-based chemodosimeter for selective gold(III) ion monitoring in aqueous media and living systems. Sensors and Actuators B Chemical 2016; 234: 109-114. doi: 10.1016/j.snb.2016.04.158.

23. Karakus E, Cakan-Akdogan G, Emrullahoglu M. A guanidinium modified rhodamine-based fluorescent probe for in vitro/vivo imaging of gold ions. Analytical Methods 2015; 7 (19): 8004-8008. doi:10.1039/C5AY01581B

24. Wang Q, Feng Y, Jiang J, Wang WJ, Chen JY et al. A coumarin-based colorimetric and fluorescent probe for the highly selective detection of Au^{3+} ions. Chinese Chemical Letters 2016; 27 (9): 1563–1566. doi: 10.1016/j.cclet.2016.02.021

25. Li Y, Qiu YX, Zhang JJ, Zhu XY, Zhu B et al. Naphthalimide derived fluorescent probes with turn-on response for Au^{3+} and the application for biological visualization. Biosensors and Bioelectronics 2016; 83: 334-338. doi: 10.1016/j.bios.2016.04.034

26. Wang W, Zhang W, Feng Y, Wang S, Lei H et al. Strategically modified highly selective mitochondria-targeted two-photon fluorescent probe for Au^{3+} employing Schiff-base: Inhibited C=N isomerization vs. hydrolysis mechanism. Dyes and Pigments 2018; 150: 241-251. doi: 10.1016/j.dyepig.2017.12.019

27. Mondal S, Manna SK, Pathak S, Ghosh A, Datta P et al. A "turn-on" fluorescent and colorimetric chemodosimeter for selective detection of Au^{3+} ions in solution and in live cells via Au^{3+}-induced hydrolysis of a rhodamine-derived Schiff base. New Journal of Chemistry 2020; 44 (19): 7954-7961. doi: 10.1039/D0NJ01273D

28. Wang J, Lin W, Yuan L, Song J, Gao W. Development of a reversible fluorescent gold sensor with high selectivity. Chemical Communications 2011; 47 (46); 12506-12508. doi: 10.1039/C1CC15086C

29. Ucuncu M, Karakus E, Emrullahoglu M. A BODIPY/pyridine conjugate for reversible fluorescence detection of gold(III) ions. New Journal of Chemistry 2015; 39 (11): 8337-8341. doi: 10.1039/C5NJ01664A

30. Silpcharu K, Samang P, Chansaenpak K, Sukwattanasinitt M, Rashatasakhon P. Selective fluorescent sensors for gold(III) ion from N-picolyl sulfonamide spirobifluorene derivatives. Journal of Photochemistry and Photobiology A: Chemistry 2020; 402: 112823-112830. doi: 10.1016/j.jphotochem.2020.112823

31. Guliyev R, Buyukcakir O, Sozmen F, Bozdemir OA. Cyanide sensing via metal ion removal from a fluorogenic BODIPY complex. Tetrahedron Letters 2009; 50: 5139-5141. doi:10.1016/j.tetlet.2009.06.117

32. Xu K, Sukhanov AA, Zhao Y, Zhao J, Ji W, Peng X, Escudero D, Jacquemin D, Voronkova VK. Unexpected nucleophilic substitution reaction of BODIPY: Preparation of the BODIPY–TEMPO triad showing radical-enhanced intersystem crossing. European Journal of Organic Chemistry 2018; 885-895. doi:10.1002/ejoc.201701724

33. Silverstein RM, Webster FX, Kiemle DJ. Spectrometric Identification of Organic Compounds. Hoboken, NJ: John Wiley & Sons, 2005.

34. Fraser RR, Renaud RN, Saunders JK, Wigfield YY. Dihedral angular dependence of H-N-C-H coupling constants. Protonated amines in trifluoroacetic acid. Canadian Journal of Chemistry 1973; 51, 2433-2437. doi: 10.1139/v73-363

Supporting Information

1. Determination of detection limit

The detection limit of BOD-AP was calculated from the fluorescence titration experiment. Initially, blank solution of BOD-AP (10 μM) was measured by 10 times and the standard deviation of these measurements was determined. Under sensing conditions, a linear relationship between the difference in fluorescence intensity and Au^{3+} ion concentration (0.2–0.8 μM) was obtained (R = 0.9976). The detection limit of BOD-AP was calculated as 17 nM based on the equation;

$$\text{Detection limit} = 3\sigma bi/m$$

where σbi is the standard deviation of blank measurements; m is the slope between intensity versus sample concentration.

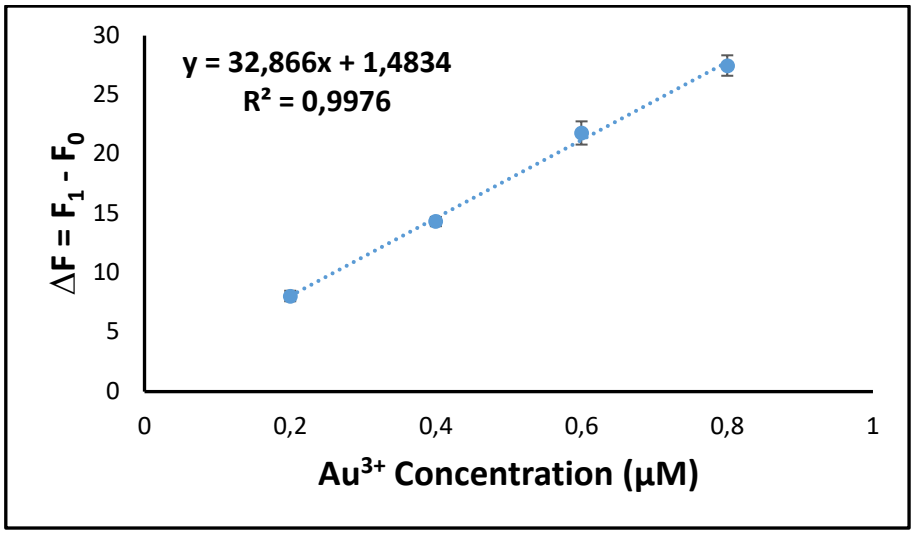

Figure S1. Fluorescence changes of BOD-AP (10 μM) upon addition of Au^{3+} (0.2 to 0.8 μM, 0.02 to 0.08 equiv.) in 0.1 M phosphate buffer, pH 7.0/EtOH (v/v, 1:1) (λ_{ex} = 460 nm, λ_{em} = 511 at 25 °C).

2. Reversibility of interaction BOD-AP with Au^{3+}

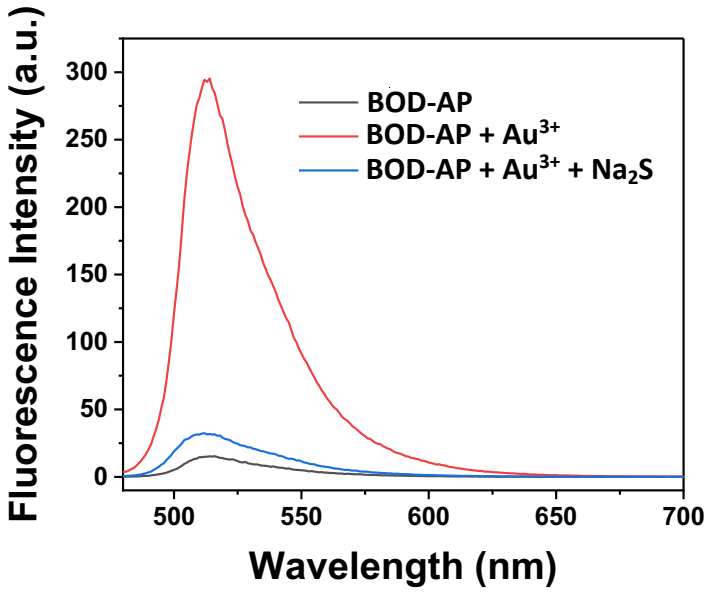

Figure S2. Fluorescence spectra of BOD-AP (10 μM) (black), BOD-AP (10 μM) + Au^{3+} (20 μM, 2 equiv.) (red), BOD-AP (10 μM) + Au^{3+} (20 μM, 2 equiv.) + Na_2S (20 μM, 2 equiv.) (blue) in 0.1 M phosphate buffer, pH 7.0/EtOH (v/v, 1:1) (λ_{ex} = 460 nm, at 25 °C).

3. Job's plot analysis of BOD-AP with Au^{3+}

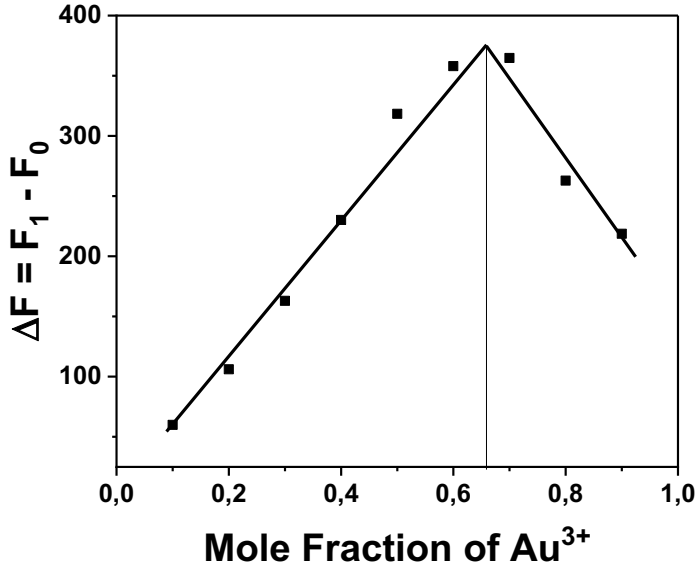

Figure S3. The Job's plot analysis between BOD-AP and Au^{3+} in 0.1 M phosphate buffer/EtOH (pH 7.0, v/v, 1:1) The total concentration of BOD-AP and Au^{3+} was kept constant at 20 μM (λ_{exc} = 460 nm, λ_{em} = 511 nm at 25 °C).

4. Selectivity of BOD-AP towards Au^{3+} in the presence of mixture of metal cations

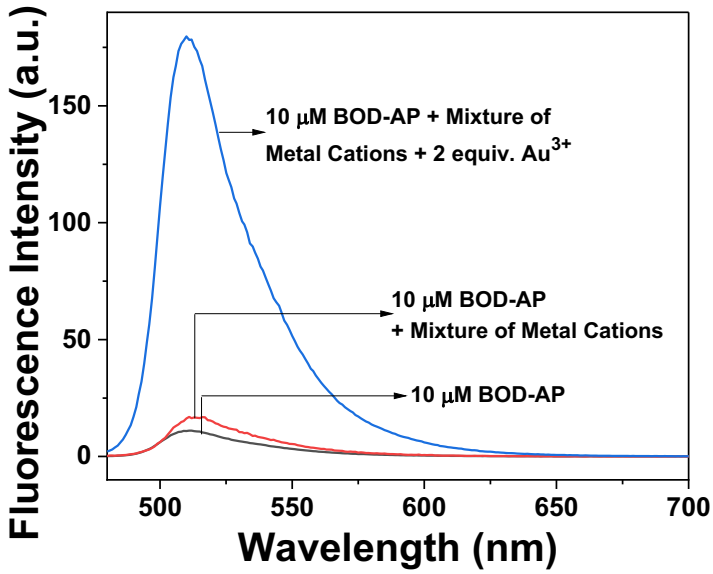

Figure S4. Fluorescence spectra of BOD-AP (10 μM) (black), BOD-AP (10 μM) + mixture of metal cations (including Na^+, K^+, Li^+, Ca^{2+}, Mg^{2+}, Ba^{2+}, Ag^+, Hg^{2+}, Zn^{2+}, Pb^{2+}, Ni^{2+}, Cd^{2+}, Fe^{2+}, Cr^{3+}, Ce^{3+}, and Al^{3+}) (100 μM, 10 equiv.) (red), BOD-AP (10 μM) + mixture of metal cations (100 μM, 10 equiv.) + Au^{3+} (20 μM, 2 equiv.) (blue) in 0.1 M phosphate buffer, pH 7.0/EtOH (v/v, 1:1) (λ_{ex} = 460 nm, at 25 °C).

5. HRMS spectrum of BOD-AP

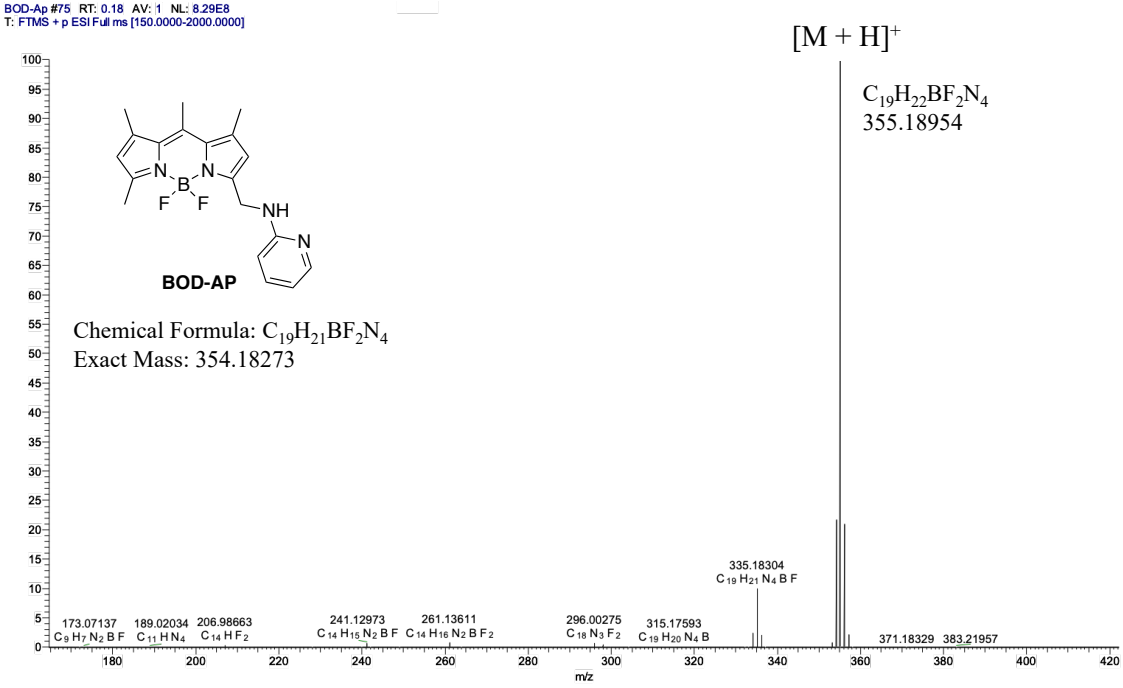

Figure S5. HRMS Spectrum of BOD-AP.

6. ^{1}H and ^{13}C NMR of BOD-AP.